NUMERICAL SIMULATION OF WHEEL-TIRE ASSEMBLY SUBJECTED TO IMPACT LOADING

R. R. V. Neves, renato.neves@gmail.com
R. C. Santiago, rafael.celeghini@gmail.com
M. Alves, maralves@usp.br
Group of Solid Mechanics and Structural Impact, Polytechnic School, University of São Paulo, Av. Prof. Mello de Moraes, 2231, São Paulo – SP, Brazil, 05508-900

Abstract. *Daily use of a car exposes the set wheel-tire to high impact loads, e.g. when colliding against curbs and road imperfections. Knowledge of the wheel-tire structural response is a first step in understanding the various mechanisms of tire compound failure. In this article, a specially design rig was developed for wheel-tire impact tests. It holds the test piece in a given position, allowing a drop mass with a round indenter to hit pressurized tires with different impact energies. A high speed camera was used to track the impact event. From the pos-processing images measurement it was possible to obtain the identer displacement and velocity. A finite element model was then conducted using material properties from the open literature. By comparing the experimental measurements and the numerical results, it became evident that the model represents well the major features of the impact of a mass on a wheel-tire assembly.*

Keywords*: tire impact, tire finite element analysis, impact experiments on tires.*

1. INTRODUCTION

Studies on the response of automotive tires subjected to impact loads are somewhat rare in the open literature. Nevertheless, it is of great importance to analyse the impact of a tire against curbs and road imperfections. Clearly, tire failure strongly affects car safety, with consequences to passengers and to the transport of goods (Orengo et al, 2003).

There are some important variables, such as tire internal pressure, impact velocity and curb geometry, that should be considered in the tire impact phenomenon (Tan et al., 2006). By taking all these variables into account, a detailed experimental programme would become rather expensive. An alternative would be to find a balance between experimental tests and numerical methods, which is the approach followed here.

A tire structure comprises a rubber matrix impregnated with reinforcement materials along its toroidal shape. Cords made of metallic, synthetic and/or natural materials interact with the low modulus of elasticity rubber compounds (Clark, 1981). The tire impact phenomenon is essentially a non-linear one given the considerable deformation and changes in the profile curvature it experiences when loaded (Mackerle, 1998). Displacements of the tire profile reach as high as 20% of its height, elongations of 40%, and interlayer shear deformation of 80% (Sokolov, 2007).

The computational solution adopted here makes use of the software ABAQUS (2007), which takes into account the geometrically and physically nonlinear behavior of the cord-reinforced rubber composite materials using the concept of rebar elements (Bolarinwa and Olatunbosun, 2004; Zamzamdeh and Negarestini, 2007; Helnwein et al, 1993). The model developed here allows the representation of different mechanical properties presented in the various regions of a tire.

In this paper an experimental set-up was developed to investigate tire-wheel assembly deformation under impact loading of a drop mass. Based on the test configuration, a finite element model was developed to analyze the stress and strength response of tire components. The displacement and velocity results were compared between numerical and experimental data. The set tire-wheel was also modeled, allowing the study of the influence of the wheel on the overall response of tires undergoing impact loadings.

2. EXPERIMENTAL PROCEDURES

Out of the shelves wheel-tire sets were rigidly fixed in a heavy support clamped to an anvil of 2.8tons. The tire is inclined by 30° to the impact mass direction so the impact region becomes restricted to the tire sidewall, Fig. 1 (a). Further, the tire platform was rotated by 35°, Fig. 1 (b). This angle was selected in such a way the impact event loads the fibers in the sidewall tire radial direction. The impact mass has at its end a round indenter, with a radius of 10mm. The final rig configuration is depicted in Fig. 1 (c).

For a given tire, no more than eight impact tests were performed, each one in a single position. Three were the variables of this study: the impact mass, the impact velocity and the tire pressure. The impact mass and velocity were chosen after several tests. The fact that there is no suspension system for the set tire-wheel reduces drastically the energy that can be used in the test with no wheel plastic deformation or tire burst (Tan et al, 2006). Accordingly, an impact mass of 47.24kg was used, with the impact velocity ranging from 2.35m/s to 5.26m/s. Nominal internal pressure value of 206.8kPa was applied to inflate the tire.

(a) (b) (c)

Figure 1. Tire impact rig. (a) angle of the tire with the vertical direction. (b) angle of the tire with the lateral face of the dropping mass. (c) indenter and the dropping mass hitting the tire.

The impact mass has a triangular shape, with and end angle of 90°. Round radius of 2mm, 10mm and 20mm were used in preliminary tests. It was found that a small radius (2mm) teared the tire with no significant deformation. Larger radius (20mm) did not fail the tire and a compromise was chosen, an indenter radius of 10mm shown in Fig. 1 (c).

A 175/65R14 radial tire and mild steel wheel of 14in (355.6mm) and 139.7mm width were used in tests.

A high speed filming camera Photron Fastcam-APX RS registered the tests at a rate of 10E3 frames per second.

2. FINITE ELEMENT MODEL

The finite element model was developed within the ABAQUS 6.7-1 enviroment, see Fig. 2. The various components of a tire were represented using the concept of rebar-layers. This allowed one to define the various mechanical properties for each component. Tab. 1 lists various details of the adopted mesh. Solid elements type C3D8R (cubic elements with 8 nodes, linear interpolation and reduced integration) were used to represent the rubber, bead core and rim.

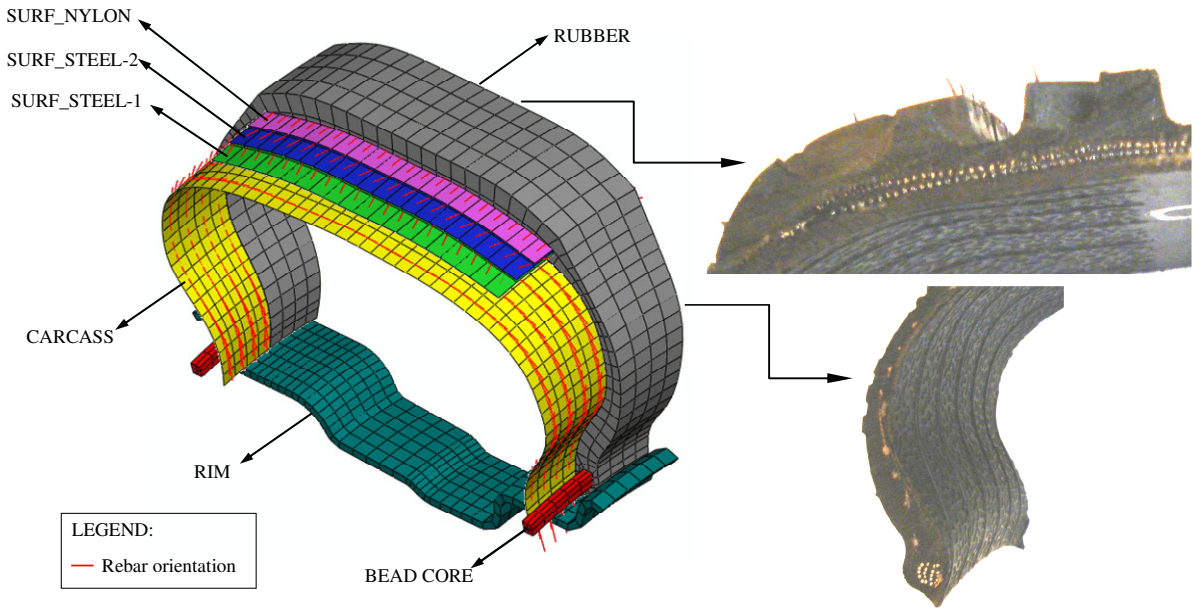

Figure 2. Finite element model of wheel-tire assembly. The reinforced belts were shown by arrows. The rebar orientation demonstrates the cords direction in each belt.

Table 1. Finite element model discretization

Region of Tire	Number of elements	Number of nodes	Element type
Rubber	27540	41400	C3D8R
Rim	9720	19800	C3D8R
Bead core	1440	3240	C3D8R
Carcass	11880	12060	SFM3D4R
Steel Belt layers (2)	7200	7560	SFM3D4R
Nylon layer	3600	3780	SFM3D4R
Identer	360	399	R3D4
Total	61740	88239	

The material model for the rubber is hyperelastic, according to the Mooney-Rivlin equation, whose deformation energy can be expressed by (ABAQUS, 2003).

$$U = \sum_{i+j=1}^{N} C_{ij} \cdot (\bar{I}_1 - 3)^i \cdot (\bar{I}_2 - 3)^j + \sum_{i=1}^{N} \frac{1}{D_i} (J_{el} - 1)^{2i} \tag{1}$$

U is the potential energy of deformation, J_{el} elastic volume rate, $\bar{I}_1$ and $\bar{I}_2$ measure the material distortion, C_{ij} describes the material shear behaviour and D_i its incompressible character, i.e. if the material is fully incompressible D_i equals zero. For N=1, one arrives at:

$$U = C_{10}(\bar{I}_1 - 3) + C_{01}(\bar{I}_2 - 3) \tag{2}$$

with the values in Tab. 2 obtained from (Bolarinwa and Olatunbosun, 2004).

Table 2. Mechanical properties of rubber

Material	C_{10}	C_{01}	Specific Mass
	N/m²	N/m²	kg/m³
Rubber	$1 \cdot 10^6$	0	940.0

The bead core is formed by 16 steel wires, total diameter of 6.4mm, whose adopted bi-linear material properties are listed in Tab. 3. The card *TIE was used for the contact between the bead core and the rubber tire.

Tab. 3 Table 3 also lists the adopted material properties for the wheel, which is assumed to be made of a low carbon steel type A36, and modeled as perfectly plastic.

The contact between the tire and the wheel is described by kinetic contact with a friction coefficient of 0.6.

Table 3. Mechanical properties of model

Material	Young's Modulus	Poisson's Ratio	Yield Tensile Strength	Ultimate Tensile Strength	Elongation at Break	Specific Mass
	N/m²		N/m²	N/m²		kg/m³
Steel belts/bead	$2 \cdot 10^{11}$	0.3	$3.5 \cdot 10^8$	$4.2 \cdot 10^8$	0.10	7850.0
Steel wheel	$2 \cdot 10^{11}$	0.3	$2.2 \cdot 10^8$	-	0.23	7850.0
Nylon	$3 \cdot 10^9$	0.3	$6.6 \cdot 10^7$	-	0.21	1140.0
Polyester	$9.5 \cdot 10^9$	0.3	$1.3 \cdot 10^8$	-	0.16	1250.0

The various nylon and steel reinforcements in the tire (SURF_STEEL-1,2 and SUR_NYLON) yield the necessary stiffness for the road-tire contact. Polyester strings radially placed are responsible for the tire geometry. The mechanical properties adopted here for these materials were obtained by (Bolarinwa and Olatunbosun, 2004). They were all modeled with the SFM3D4R finite element, whose geometric properties are listed in Tab. 4. The interaction between the reinforcement strings and the tire rubber was defined using the *EMBEDDED ELEMENT constraint.

Table 4. Geometric properties of reinforcement materials

Surface	Cross Sectional Area	Spacing	Orientation
	mm²	mm	°
SURF_STEEL-1	0.19630	1.28	20
SURF_STEEL-2	0.19630	1.28	-20
SURF_NYLON	0.42084	1.19	0
SURF_CARCASS	0.42084	1.00	90

The indenter was modeled as a rigid element, R3D4, with the drop mass attached to a reference point. Except for the free fall direction, motion was restricted in all directions for the indenter. Contact was defined between the tire and the indenter.

A gravitational acceleration of 9.23m/s² was applied to the impact mass to compensate for friction in the guides of the drop hammer used in the actual experiment. Figure 3 shows some details of the model, together with the clamped boundary condition applied to wheel.

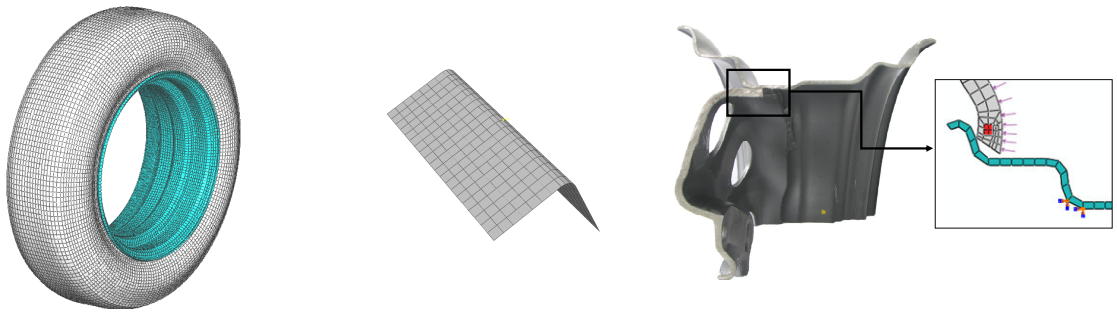

(a) (b) (c)

Figure 3. (a) Finite element mesh of tire-wheel assembly; (b) indenter mesh; (c) loads and boundary conditions applied in the model

4. RESULTS

One experiment was performed at an impact velocity of 5.26 m/s and drop mass of 47.24 kg, with the tire inflate to 206.8 kPa. These initial conditions lead to a typical failure of the tire in the most compressed region, between the indenter and the rim. Fig. 4 depicts images of the impact event, where rubber tearing and wheel plastic deformation are evident.

Using the **ImageJ** program for image analysis it was possible to obtain the indenter displacements during the impact event. These data were then processed to give the velocity of the dropping mass during the impact event. A comparison between the simulation and the experimental data for mass velocity is given in Fig. 5.

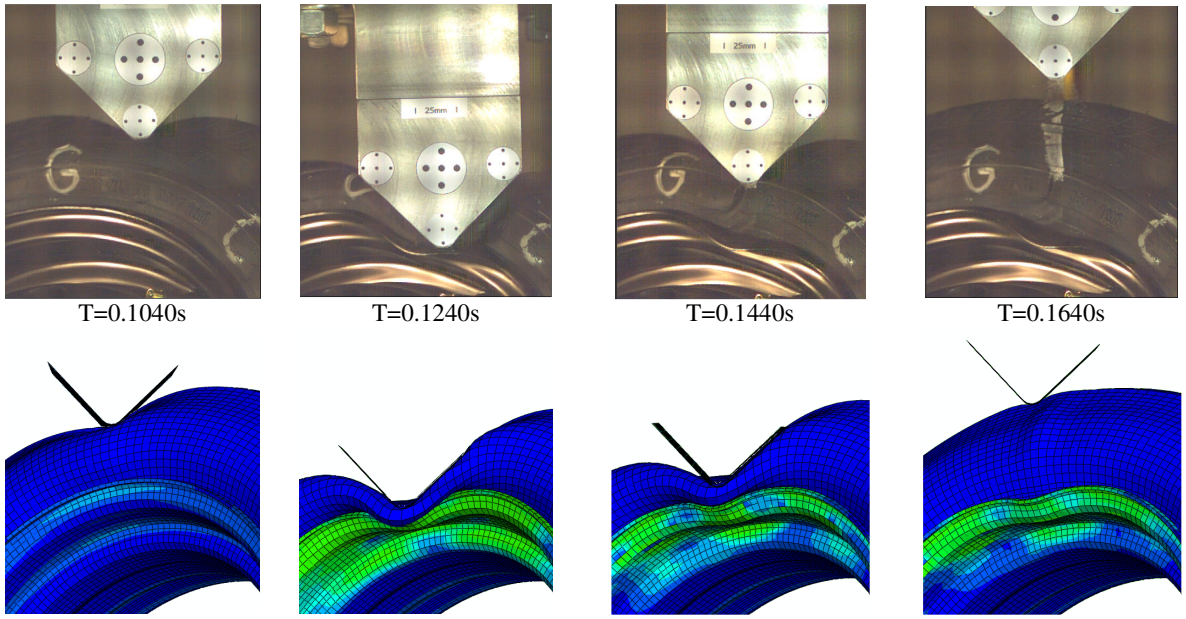

Figure 4. Comparison of simulation and video images from the impact event.

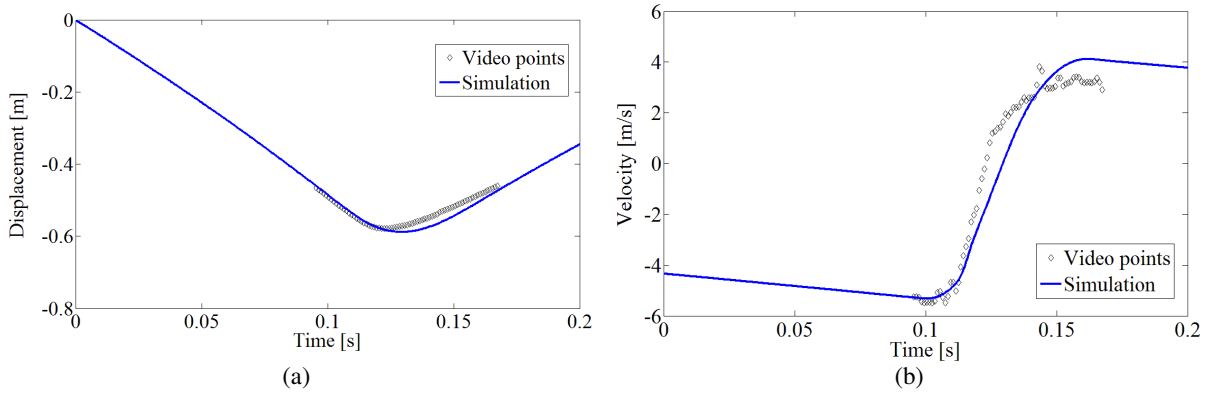

Figure 5. Displacement (a) and velocity (b) of the impact mass.

Fig. 6 shows the wheel-tire assembly region affected by collision at the maximum displacement of the drop mass. The tire section represented in Fig. 6 is similar to the one in Fig. 2. It can be seen the presence of higher tensions values in the bead core and in the two steel cord-reinforced plies. The associate rim deformation is shown in Fig. 7.

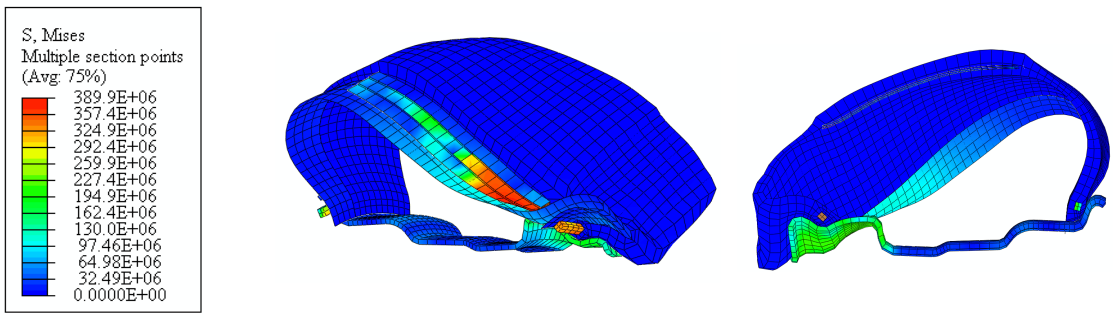

Figure 6. Von Mises stress on tire impact region at maximum deformation – scale factor 1 and units at N/m².

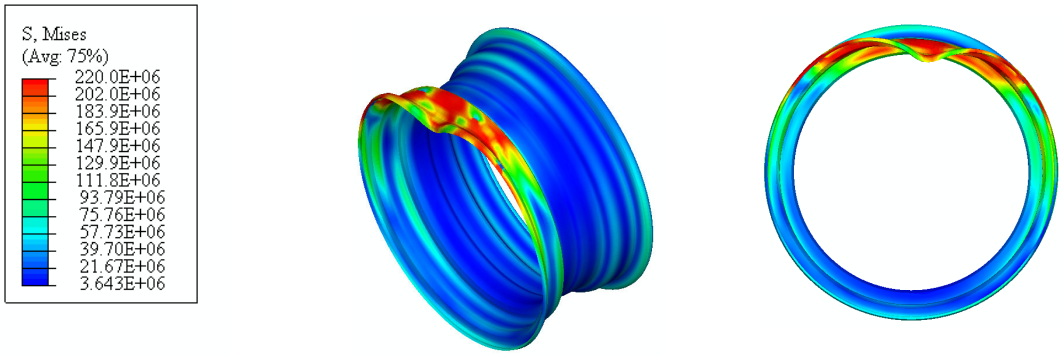

Figure 7. Results of Von Mises stress on the rim at maximum deformation – scale factor 1 and units at N/m².

5. DISCUSSION

Fig. 4 indicated the good correlation between the experiments and simulation. The impact conditions analyzed at this test are critical. The rubber cut extended throughout the carcass, resulting in air leakage and loss of pressure. The simulation shows that the rubber is compressed against the rim, leading to its permanent deformation. Tire sidewall demonstrates also a swelling surface, like a blister. No failures properties were applied to the finite element model.

The image analysis was performed by picking 73 points trough the impact event using a 0.001s constant interval. These data were compared with simulation results in Fig. 5 (a). The maximum difference of 28.35mm was observed at 0.1445s, a deviation of 5.04%.

It's evident from Fig. 6 that the cord-reinforced belts support the major impact force applied onto the tire. The maximum stress at 389.9MPa in SURF_STTEL-1 and 377.7MPa at SURF_STTEL-2 indicate plastic deformation according to the properties adopted. The bead core at impact region is under a similar state. SURF_NYLON experiences a stress of 65.9MPa, close to its limit. The stress values in the rubber matrix are around 6.3MPa, one sixty times smaller than the steel cords stress. The stress in the carcass, of 122.3MPa, is not enough to cause its yielding, even at its maximum deformation.

6. CONCLUSIONS

In real use, tires are submitted to adverse road conditions that may cause transient dynamic loading events. The proposed model was developed to analyze such impact events. It has the capability to be used for the analysis of phenomena like collision with obstacles, holes and bumps.

Good correlation between experimental and numerical data was achieved. This allowed one to infer the magnitude of important variables with a good degree of confidence. The fact that the rim was considered in the simulation allows one to explore further the phenomenon of failure of tires.

7. REFERENCES

ABAQUS, 2003, "ABAQUS user's manual version 6.4". Abaqus Inc.

ABAQUS, 2007, "An integrated approach for transient rolling of tires". Abaqus Technology Brief.

Bolarinwa, E. O., Olatunbosun, O., 2004, "Finite element simulation of tire burst test". Proc. Instn Mech. Engrs , 218, 1252-1258.

Clark, S. K., 1981, "Mechanis of pneumatic tires". Washington, D.C., U.S.: Department of Transportation National Highway Traffic Administration.

Helnwein P., Liu, C., Meschke, Mang, H. A., 1993, "A new 3-D finite element model for cord reinforced rubber composites - Application to analysis of automobile tires". Finite Elements in Analysis and Design , 14, 1-16.

Mackerle, J., 1998, "Rubber and rubber-like materials, finite-element analyses and simulations: a bibliography (1976-1997)". Modelling Simulation Material Science Engineering , *6*, 171-198.

Orengo F., Ray, M., Plaxico, A., 2003, "Modelling tire blow-out in roadside simulation using LS-DYNA". ASME International Mechanical Engineering Congres & Exposition IMECE .

Sokolov, S., 2007, "Calculation of the stress-strain atate of pneumatic tires by the finite element method". Journal of New Technologies in Machinery Manufacture Reliability , 36, 45-49.

Tan, K. S., Wong, S. V., Radim Umar, R.S., 2006, "An experimental study of deformation behaviour of motorcycle front wheel-tire assembly under frontal impact loading". International Journal of Impact Engineering , 32, 1554-1572.

Zamzamdeh M, Negarestini, M., 2007, "A 3D tire/road interaction simulation by a developed model (ABAQUS-code)". ASIMMOD .

5. RESPONSIBILITY NOTICE

The author(s) is (are) the only responsible for the printed material included in this paper.